Electronic properties of cubic and hexagonal SiC polytypes from *ab initio* calculations

P. Käckell, B. Wenzien, and F. Bechstedt
Friedrich-Schiller-Universität, Institut für Festkörpertheorie und Theoretische Optik, Max-Wien-Platz 1, 07743 Jena, Germany
(Received 21 April 1994)

Ab initio total-energy studies are used to determine the lattice constants and the atomic positions within the unit cells for 3*C*-, 6*H*-, 4*H*-, and 2*H*-SiC. The electronic structures are calculated for the atomic geometries obtained theoretically within the density-functional theory (DFT) and the local-density approximation (LDA). We state more precisely the ordering of the conduction-band minima and derive effective masses. By adding quasiparticle corrections to the DFT-LDA band structures we find indirect fundamental energy gaps in agreement with the experiment. A physical explanation of the empirical Choyke-Hamilton-Patrick relation is given. Band discontinuities, bandwidths, crystal-field splittings, and ionic gaps are discussed versus hexagonality.

I. INTRODUCTION

The physics of silicon carbide and the possibilities of its use in devices have been subjects of considerable interest because of its strong chemical bonding, physical stability, and other attractive electrical, optical, and thermal properties. Many applications require a detailed knowledge of the electronic structure of the material, which itself depends on the atomic geometry. The latter one is rather complicated since SiC crystallizes in more than hundred different modifications, i.e., polytypes. The band structure of SiC and, in particular, the indirect fundamental gap vary remarkably with the polytype.[1]

In numerous theoretical studies in the last twenty years *ab initio* pseudopotential methods are extensively applied to the ground-state properties of 3*C*-SiC,[2–6] 2*H*-SiC,[7–10] and also 4*H*- or 6*H*-SiC.[8–11] However, results of *ab initio* density-functional-theory (DFT) calculations based on the local-density approximation (LDA) for the electronic structure are only available for 3*C* (Refs. 12–14) and 2*H* (Refs. 12 and 14) polytypes. Only in a very recent work[15] also 4*H* and 6*H* have been studied. However, the DFT-LDA band gaps of semiconductors and insulators have been consistently underestimated by 30–50% compared with the experiment.[16–18] Despite the discrepancies between the calculated and measured band gaps, the dispersion of single bands as well as the energetical ordering of the conduction-band minima come out nearly correctly from the calculations. When many-body quasiparticle (QP) effects[16,18] are taken into account additionally, a reliable indirect energy gap may be predicted, at least for cubic 3*C*-SiC.[17,19,20]

The majority of the *ab initio* DFT-LDA calculations concerning SiC (Refs. 2–5 and 7–15) expand the wave functions in terms of plane waves. The only exception concerns the full-potential linear-muffin-tin-orbital (LMTO) method.[6] In the case of electronic-structure LMTO calculations for SiC polytypes usually the semiempirical atomic-sphere approximation (ASA) is additionally introduced.[21–24] In general, the gap problem appears also within the LMTO-ASA description. However, it is remarkably reduced by varying the number and the radii of the atomic spheres for the different polytypes.[21,23] Electronic band structure studies for zinc-blende and wurtzite SiC before 1987 have applied empirical methods, e.g., the empirical pseudopotential method[25,26] or semiempirical linear combination of atomic orbitals methods.[27–29] Recently, Backes *et al.*[30] suggested an interesting interpretation of the trends in the electronic structure versus the polytype by considering the polytypes as structures of mutually twisted Si-C bilayers and by interface matching of the electronic wave functions. More or less direct experimental studies of the electronic structure of the SiC polytypes are rather rare. Besides x-ray emission spectra[31,32] only one band structure mapping[33] exists for 3*C*-SiC.

In the present paper, we present results of parameter-free pseudopotential calculations. The lattice constants a, c (for the hexagonal polytypes 2*H*, 4*H*, and 6*H*), or the length a_0 of the characteristic cube (for zinc-blende 3*C*-SiC) are determined by means of total-energy minimizations. The atomic positions within the hexagonal unit cells are also optimized.[11] Then, the band structures are calculated for the theoretical equilibrium atomic structures. Otherwise, polytypes under pressure would be considered.[34] The influence of the atomic relaxations within the unit cells on the electronic structure is discussed. We study the dispersion of the resulting bands in more detail. The energetical ordering of the conduction-band minima is studied versus the "percentage hexagonality" of the polytypes. We discuss reasons for the indirectness of the energy gaps. With the physical explanation of the linear relation between the electronic energy gap and the percentage hexagonality up to 50%, i.e., the Choyke-Hamilton-Patrick rule,[1] a long-standing, but unresolved problem is attacked. Furthermore, the resulting effective masses are compared with experimental results and their structural trends are derived.

II. THEORETICAL INPUT

In our DFT-LDA theory, the electron-ion interaction is treated by using norm-conserving, *ab initio* pseudopotentials of the Bachelet-Hamann-Schlüter (BHS) type[35] in the fully separable Kleinman-Bylander form.[36] Within the applied self-consistent method, the electron wave functions are expanded in terms of plane waves. The number of plane waves in this expansion is determined by the energy cutoff. In the beginning, the norm-conserving pseudopotentials are generated for Si and C atoms according to the data of Ref. 37, giving rise to potentials similar to the BHS ones.[36] Unfortunately, for this choice of the carbon pseudopotentials the energy cutoff should be rather large, about 80 Ry or more, to reach convergency in the ground-state and electronic properties, due to the lack of core p states. Therefore, we use the degrees of freedom that one has in generating pseudopotentials[10,11,38] to our advantage by carefully choosing the core radii r_c for carbon, outside of which true and pseudowave functions are identical.[36,37] Enlarging r_c means softening of the pseudopotentials, i.e., a smaller number of plane waves is required. In the BHS type potentials, r_c is determined by a parameter cc_l; more strictly by $r_c = r_{\max}/cc_l$, where $r_{\max}$ is the position of the outermost peak in the all-electron wave function and l denotes the quantum number of the angular momentum. We generate pseudopotentials for angular momentum components $l = 0, 1$, and 2. The corresponding parameters for carbon are $cc_s = 1.7$ and $cc_p = 1.6$. They are somewhat smaller than the BHS values $cc_s = 1.8$ and $cc_p = 3.0$. The d potential, which plays the role of the local part, has not been modified. For silicon we use the pseudopotentials given in Ref. 37. In the case of $3C$-SiC it is clearly shown in Ref. 10 that the convergency of the physical quantities is much more rapid with respect to the energy cutoff if the modified carbon pseudopotentials are applied. Therefore the energy cutoff may be reduced to a reasonable value of about 34 Ry.

Performing the self-consistent DFT-LDA calculations we apply the computer code `fhi93cp` of Stumpf and Scheffler.[39] In a first step both the hexagonal lattice constants a and c and the atomic geometries within the unit cells of the hexagonal polytypes are relaxed until the Hellmann-Feynman forces vanish and the total energy reaches a minimum, using a steepest-descent method together with a Car-Parrinello-like approach[40] for bringing the wave functions to self-consistency. In the $3C$-SiC case the procedure reduces to the variation of only the cubic lattice constant a_0. The $\mathbf{k}$ integration is replaced by a sum of special $\mathbf{k}$ points in the irreducible part of the Brillouin zone (BZ). The special $\mathbf{k}$ points are generated according to Chadi and Cohen[41] using the special scheme of Evarestov and Smirnov.[42] We apply six mesh points in the hexagonal case. The many-body electron-electron interaction within LDA is described by the Ceperley-Alder scheme[43] as parametrized by Perdew and Zunger.[44]

The geometrical structures of the polytypes, at which the band structures are calculated, are represented in Table I. They are derived from total-energy and force minimizations.[11] The lattice constants a and c result from finding the minimum of the total energy with respect to a and c, whereas the atomic positions within the hexagonal unit cells result from the vanishing Hellmann-Feynman forces. The atomic positions can be represented by triples in terms of the three primitive vectors of the hexagonal Bravais lattice.[11,45] The coordinates in the planes perpendicular to the c axis are only defined by the lattice constant a. The coordinates u, v, and w parallel to the c axis can be expressed by the constant c. In the pH polytypes ($p = 2, 4, 6$) they vary only in the first $j = 1, ..., p/2$ Si-C bilayers. For the silicon and carbon atom in these bilayers it holds $u(\mathrm{Si}) = 0$ and $u(\mathrm{C}) = \frac{3}{8} + \varepsilon(1)$ for $2H$; $u(\mathrm{Si}) = 0$, $u(\mathrm{C}) = \frac{3}{16} + \varepsilon(1)$, $v(\mathrm{Si}) = \frac{1}{4} + \delta(2)$, and $v(\mathrm{C}) = \frac{7}{16} + \varepsilon(2)$ for $4H$; and $u(\mathrm{Si}) = 0$, $u(\mathrm{C}) = \frac{1}{8} + \varepsilon(1)$, $v(\mathrm{Si}) = \frac{1}{6} + \delta(2)$, $v(\mathrm{C}) = \frac{7}{24} + \varepsilon(2)$, $w(\mathrm{Si}) = \frac{1}{3} + \delta(3)$, and $w(\mathrm{C}) = \frac{11}{24} + \varepsilon(3)$ for $6H$. The other coordinates follow from the space-group symmetry C_{6v}^4.

The $(p-1)$ independent dimensionless cell-internal parameters are also listed in Table I. They indicate the deviations from the atomic positions in an ideal tetrahedral structure with $c/(pa) = \sqrt{2/3}$. Without loss of generality, $\delta(1) \equiv 0$ is chosen. As typical for DFT-LDA calculations without the inclusion of the zero-point atomic displacements, the lattice constants in Table I are somewhat underestimated by about 1% in comparison to the experimental values.[45–48] The internal geometry of the hexagonal unit cells is however in reasonable agreement with results of x-ray studies,[47,49] in particular for $6H$. Despite the small deviations from the experimental geometries we start from the atomic structures derived theoretically, because they are stress free.

The used DFT-LDA well describes the ground-state properties of the polytypes. However, it can hardly

TABLE I. Theoretical hexagonal lattice constants and cell-internal parameters of the considered SiC structures. p denotes the number of the Si-C bilayers in the unit cell of the pC or pH polytype.

Polytype	a (Å)	c/p (Å)	Layer j	$\varepsilon(j)$	$\delta(j)$
$3C$	3.034	2.477			
			1	0.000 37	0.000 00
$6H$	3.033	2.480	2	0.000 06	0.000 03
			3	–0.000 09	–0.000 12
$4H$	3.032	2.482	1	0.000 48	0.000 00
			2	–0.000 23	–0.000 21
$2H$	3.031	2.480	1	0.000 80	0.000 00

be applied to derive electronic excitation energies from the resulting energy band structures. Energy gaps and transition energies are remarkably underestimated. These underestimations in comparison to experimental values can be removed by adding many-body QP corrections.[16–20] We assume that in general they give rise to a nearly rigid shift of the empty bands against the occupied valence bands. The rigid shift is identified with the QP correction for the fundamental energy gap. A simplified analysis of Bechstedt and Del Sole[18,19] of the QP self-energy within Hedin's GW approximation[16,50] gives a simple analytic expression for the correction $\Delta_{\rm QP}$ to the DFT-LDA band gaps,

$$\Delta_{\rm QP} = e^2 q_{\rm TF}/\epsilon_\infty/(1 + 7.62 q_{\rm TF} r_0), \qquad (1)$$

where the high-frequency dielectric constant ϵ_∞ and the Thomas-Fermi wave number $q_{\rm TF}$ characterize the screening properties of the system. The radius r_0 denotes the averaged decay constants of the valence-electron wave functions of the anion and the cation. Using expression (1), reasonable gap corrections may be estimated,[14,19,22,24] at least for zinc-blende SiC. With the cation and anion radii from Ref. 18, the bond polarizability as defined by Harrison,[51] the lattice constant (cf. Table I), and the dielectric constant[51] we find a value $\Delta_{\rm QP}$=1.13 eV. The small variations from polytype to polytype are neglected in the following. The variations of the electron density are negligible since the changes of the Si-C pair volumes between the polytypes are extremely small.[11] The splitting of the high-frequency dielectric constants parallel and perpendicular to the c axis in $6H$ amounts less than 3% of the constant for $3C$.[48] The resulting shift variations of about 0.03 eV with the polytype are neglected in our estimation.

III. RESULTS AND DISCUSSION

A. Band structures

The resulting DFT-LDA band structures are represented in Fig. 1 versus high-symmetry lines A-L-M-Γ-A-H-K-Γ within the BZ of the hexagonal system. For direct comparison we present the cubic structure in a hexagonal $3H$ cell. The zero of the pseudopotentials is used as the energy zero for all polytypes. The hexagonal BZ is shown in Fig. 2. The overall features of the band structures agree well with previous calculations.[12–15,20–29] The top of the occupied valence-band states is situated at Γ. Differences concern the magnitude of the various band gaps, where this effect is not only related to their underestimation within DFT-LDA. Rather, there are variations in the position of the conduction-band minima. Surely, the minimum in the wurtzite structure $2H$-SiC is located at the K point in the center of the BZ edge parallel to the c axis similarly to hexagonal diamond.[52] The X point in the fcc BZ represents the position of the minimum in the zinc-blende $3C$-SiC. Two of these X points are folded onto M points of the hexagonal BZ of the corresponding $3H$ structure. The exact positions depend on the details of the calculations, the ratio c/a of the hexagonal lattice constants, as well as the atomic positions within the hexagonal unit cells. For the relaxed structures we find the conduction-band minima at M for $4H$ and, respectively, at about $0.63LM$ for $6H$. This result is somewhat surprising since the fcc X point should map onto $\frac{1}{3}LM$ for $4H$and M for $6H$. That means that the simplifying folding argument is not exactly valid going from one polytype to another one. The actual arrangement of atoms and bonds in the unit cells gives rise to changes in the band position and dispersion. The exact minimum position is particularly sensitive to the details of the atomic

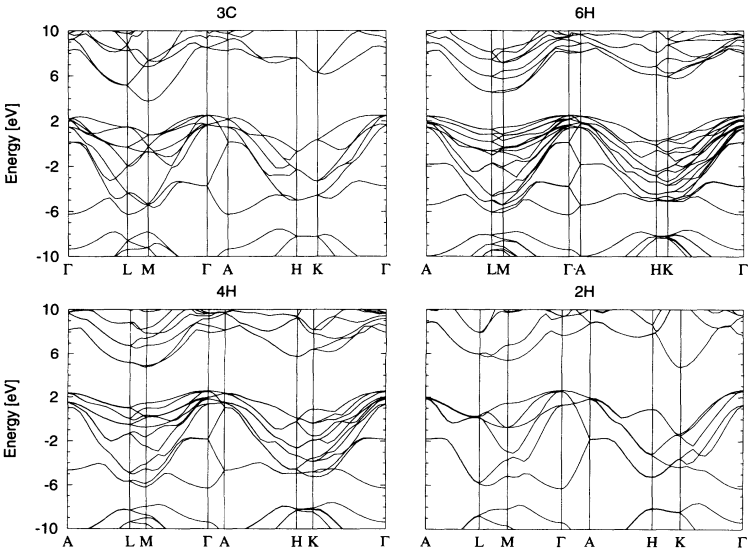

FIG. 1. Band structures for $3C$-, $6H$-, $4H$-, and $2H$-SiC.

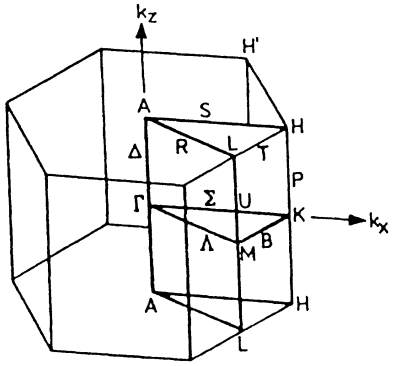

FIG. 2. Brillouin zone of the hexagonal lattice.

structure since the lowest conduction band between L and M is rather flat. This flatness increases with the lowering of the LM distance in $\mathbf{k}$ space. Hence the $6H$ case is the most critical one.

The general findings that all considered polytypes are indirect semiconductors are not surprising, including that the conduction-band minimum is located at X in the zinc-blende structure or at M in the hexagonal BZ of $3H$. Diamond and silicon show a similar behavior, there the conduction-band minima are situated on the ΓX line near X. Moreover, the upper valence band has the lowest energy in X, so that the repulsive interaction between the lowest conduction band and the highest valence band should be small. In the wurtzite structure, the situation is changed. First of all, the zinc-blende X is folded onto $\frac{2}{3}LM$ in the hexagonal BZ of $2H$. This point has a lower symmetry and the bonding and antibonding combinations of the C $2s$ orbital and a Si $3p$ orbital, of which the state mainly consists, can interact with more closer lying states. The minimum at K, that has a similar orbital character as the states at the zinc-blende W, gives rise to the lowest empty band. On the other hand, going from $2H$ to $4H$ or $2H$ to $6H$, H (L) maps onto K (M) or onto $\frac{2}{3}HK$ ($\frac{2}{3}LM$) (cf. Fig. 1). The energetical distance of the valence and conduction bands in K is remarkably reduced. The resulting stronger interaction pushes the conduction-band minimum away from the valence bands. States on the LM line near M form the lowest conduction-band minimum.

B. Transition energies and band discontinuities

The behavior of the conduction-band extrema as well as the highest valence band with the polytype can be seen from Table II. For comparison in this table, the $3C$ band structure is represented within a $3H$ BZ and the most important high-symmetry points Γ, K, H, A, M, and L in the hexagonal BZ are considered. In addition, the resulting indirect energy gaps are also given. Some of these energies show a clear trend with the hexagonality of the polytypes. The monotonic behavior is only disturbed by the K_{2c} level in the $4H$ structure. The Γ_{1c} and K_{2c} energy levels decrease with rising hexagonality, whereas the M_{1c} conduction-band minimum shows the reverse trend. The increase of the Γ_{1c} level with decreasing hexagonality is perhaps somewhat overestimated. We find a value for the direct energy gap at Γ in $3C$-SiC that is larger than the corresponding experimental value.[48] This is suprising, since we expect a general underestimation of the transition energies within DFT-LDA. However, such an overestimation is also stated by other authors[12,15,20] using a similar calculational method. In the zinc-blende $3C$ case one finds within the DFT-LDA larger transition energies $\Gamma_{15v} \rightarrow \Gamma_{1c}$ and $\Gamma_{15v} \rightarrow L_{1c}$ as observed experimentally. However, the most experimental transition energies have been obtained from reflectivity measurements. Therefore, the discrepancies can arise from an incorrect identification of the high-symmetry point in the experimental analysis. In general, the conduction-band minimum at Γ is much higher in energy than the minima at M and K. There seems to be practically no chance to prepare a SiC polytype, showing a direct gap with a reasonable oscillator strength, apart from a certain stronger rearrangement of the Si and C atomic layers, leaving the SiC material class.

The most interesting aspect of the band structures is related to the magnitude and the location in the BZ of the fundamental indirect energy gap E_g^{ind} versus the polytype or the corresponding percentage hexagonality. The relevant trends are represented in Fig. 3 for the gaps $\Gamma_{6v} \rightarrow M_{1c}$ (or, respectively, conduction-band states between $L_{1/3c}$ and M_{1c}) and $\Gamma_{6v} \rightarrow K_{2c}$. The transition energies are compared with experimental data for the indirect gaps.[48] They exhibit a linear increase from 0% ($3C$-SiC) to 50% ($4H$-SiC) and a nearly constant behav-

TABLE II. Density-functional theory–local-density approximation energies of the lowest conduction band and the highest valence band at high-symmetry points in the hexagonal BZ. The zinc-blende structure is calculated within a $3H$ cell. The VBM is used as energy zero. In addition, the indirect gaps are given.

Polytype	Γ	K	H	A	M	L	E_g^{ind}
$3C$	5.99	3.78	5.08	5.74	1.27	2.66	1.27
	0.00	−2.19	−3.20	−0.32	−1.76	−1.03	
$6H$	5.49	3.41	3.59	5.55	1.98	2.01	1.96
	0.00	−2.06	−2.27	−0.08	−1.08	−1.29	
$4H$	5.40	3.88	3.15	5.60	2.18	2.59	2.18
	0.00	−1.65	−2.47	−0.19	−1.11	−1.53	
$2H$	5.07	2.10	5.21	6.15	2.72	3.31	2.10
	0.00	−3.93	−1.69	−0.68	−1.17	−2.31	

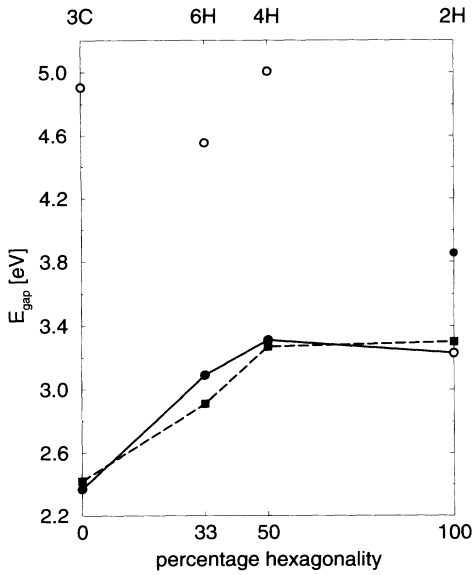

FIG. 3. Relevant indirect band gaps $\Gamma_{6v} \rightarrow M_{1c}$ (or between $L_{1/3c}$ and M_{1c}) and $\Gamma_{6v} \rightarrow K_{2c}$ versus the percentage hexagonality. Theoretical results are marked by full and open circles. For comparison experimental results (Ref. 48) are plotted as squares and connected by dashed lines, whereby in the case of $2H$ and $4H$ the excitonic gap energies are taken. The lowest theoretical gaps are connected by solid lines.

ior between 50% and 100% ($2H$-SiC). This behavior is represented by the empirical Choyke-Hamilton-Patrick (CHP) rule.[1] For comparison with the experiment the DFT-LDA values are enlarged by the QP gap correction $\Delta_{QP} = 1.13$ eV according to expression (1). One obtains two interesting results. First, the interplay of the two indirect transitions $\Gamma \rightarrow M$ and $\Gamma \rightarrow K$ explains the CHP rule. For not too large hexagonality the fundamental indirect gap is related to $\Gamma \rightarrow M$ (or near M) transitions, resulting in a linear behavior. In the case of the wurtzite structure, the energy of the $\Gamma \rightarrow K$ transitions is smaller than that of the $\Gamma \rightarrow M$ ones, giving rise to the seemingly constant gap going from $4H$ to $2H$. Second, the DFT-LDA values for the lowest indirect gaps increased by Δ_{QP} give rise to values close to the experimental ones. The agreement between theoretical and experimental indirect gaps is reasonable. Small deviations may be traced back to variations in the QP gap correction and the exciton binding energy with the polytype. Thereby, the DFT-LDA results are nearly independent on details of the calculational method. Denteneer[53] finds similar DFT-LDA gap energies for $2H$-, $4H$-, and $3C$-SiC.

Three quantities which characterize the valence band structure are given in Table III. They are the total width of the valence bands W, the ionic gap E_g^{ion} within the valence bands, and the splitting Δ_{cryst} of the threefold degenerated valence-band maximum (VBM) of zinc blende into a twofold (p_x and p_y) Γ_{6v} VBM and a lower one-fold (p_z) Γ_{1v} splitoff band of the hexagonal pH polytypes by the hexagonal crystal field. The total valence-band widths of cubic and hexagonal SiC polytypes are similar. There is only a slight increase of W with the

TABLE III. Valence-band parameters (width W, ionic gap E_g^{ion} at $\frac{2}{3}\Gamma K \rightarrow \Gamma$, crystal-field splitting Δ_{cryst}) and band discontinuities [ΔE_v and ΔE_c with respect to $3C$ (but calculated in $3H$)] for the SiC polytypes. All values in eV, apart from Δ_{cryst} (in meV).

Polytype	W	E_g^{ion} (M)	Δ_{cryst}	ΔE_v	ΔE_c
$3C$	15.64	1.32	0	0.00	0.00
$6H$	15.69	1.33	36	−0.02	0.74
$4H$	15.72	1.33	56	−0.05	0.99
$2H$	15.81	1.32	97	−0.13	0.99

percentage hexagonality. Both the absolute magnitude and the variation with the polytype are comparable with other DFT-LDA observations.[15] The averaged ionic gap between the p lowest valence bands and the $3p$ higher valence bands in pH (for zinc blende it holds $p = 1$ in this case) is a measure of the ionicity of the chemical bonds in the system. However, the considered indirect ionic gap $\frac{2}{3}\Gamma K \rightarrow \Gamma$ exhibits no clear variation with the hexagonality. That indicates the near constancy of the ionic character of the bonds versus the polytypes.

When the hexagonal stacking nature is enhanced from $3C$, $6H$, $4H$ to $2H$, the crystal-field splitting Δ_{cryst} of the upper valence bands increases enormously. In the hexagonal cases it is much larger than the experimental spin-orbit splitting of 7–10 meV.[54] The values for Δ_{cryst} listed in Table III measure the differences in the electron densities of hexagonal and cubic Si-C bilayers in the different stacking sequences parallel to the hexagonal axis ([111] or [0001]) apart from the effect of the 60° rotating of the hexagonal layers against the cubic ones. They therefore grow with rising hexagonality h.

An interesting problem concerns the preparation of heterostructures on the base of chemically identical, but structurally inequivalent semiconductors, more strictly speaking of different polytypes. The key parameters of such structures are the band offsets at the interface. We have calculated the discontinuities using the energy zero of the atomic pseudopotentials as the reference level of the alignment. An influence of QP effects on the offsets is neglected, assuming that the QP shifts for the VBM and the conduction-band minimum (CBM) are nearly independent of the polytype. We have also checked the alignment of the averaged electrostatic potentials. The results are the same since the potentials vary only by a few meV.

Results for the VBM at Γ (ΔE_v) and the CBM at near M, M, or K (ΔE_c) are also listed in Table III. They are referred to the band edges of the zinc-blende SiC calculated within the $3H$ structure. The results seem to indicate type-II heterostructures for the considered combinations, i.e., electron wells are located in the zinc-blende material whereas hole wells appear in the hexagonal layers. However, the valence-band discontinuities ΔE_v are so small that in any case we expect rather flat hole wells considering the width of the fundamental gap. The band discontinuities in Table III are confirmed by a recent tight-binding estimation[55] that derived $\Delta E_v = -0.146$ eV for a $3C/2H$ heterostructure. For a $3C/6H$ combina-

tion our values agree well with predictions of $\Delta E_v = 0$ eV and $\Delta E_c = 0.66$ eV by Mönch[56] in the framework of the electronegativity concept. On the other hand, we observe remarkable offsets for the conduction bands ΔE_c. The corresponding values increase with the hexagonality in a similar manner as the indirect gaps. It seems to be noteworthy to mention, that reasonable values for ΔE_c also result for heterojunctions formed by two hexagonal polytypes. For instance, it holds $\Delta E_c \approx 0.3$ eV for a $4H/6H$ combination. That means, even at such interfaces a two-dimensional electron gas can appear. The occurrence of a type-II heterostructure in the $3C/pH$ case is related to the indirectness of the studied semiconductors. Considering also the conduction-band minima in Γ the electron wells would also appear in the hexagonal material layers. The character of such a heterostructure would, however, be of type I.

C. Effective masses

In general, we expect that the DFT-LDA nearly gives the principal curvature of the energy bands. This should be also true near the extreme $\mathbf{k}$ of the band structure within the BZ. Therefore we try to derive components of the effective-mass tensors $m_{ij}(\mathbf{k})$ from our calculations using the second derivatives of the bands. Results for the lowest conduction-band minima in K, M, or at the LM line near M are given in Table IV. For electrons we give the full inverse effective-mass tensor along the principal axis determined by the c axis of the structure and the position of the minimum in $\mathbf{k}$ space. We consider the longitudinal masses $m_{||}$ parallel to the connection line between the minimum position and Γ, more strictly speaking parallel $M\Gamma$ ($4H$, $3H$), $K\Gamma$ ($2H$), and $(LM)\Gamma$ ($6H$). The two transverse masses $m_{\perp 1}$ and $m_{\perp 2}$ are distinguished according to the anisotropy of the system. $m_{\perp 1}$ denotes the transverse mass parallel to the c axis. In the calculation of $m_{\perp 1}$ we use the direction ML. For the estimation of the second transverse mass $m_{\perp 2}$ of the hexagonal polytypes we replace the correct direction by the line MK in an approximate manner. For comparison the zinc-blende SiC polytype is also calculated within a hexagonal $3H$ structure.

No clear trend with the hexagonality or the extent of the unit cell can be derived from Table IV for the electron masses. This is not astonishing since the conduction-band minima appear at different $\mathbf{k}$ points in the BZ. Only in the $3H$ and $4H$ cases one observes the minimum at the same point M. A remarkable anisotropy of the electron effective-mass tensor is found for $6H$ and $4H$. In space directions (nearly) parallel to $M\Gamma$ and $L\Gamma$ heavy electrons appear whereas the mass for the electron motion in the plane perpendicular to c axis but parallel to the edge MK of the hexagonal BZ is small. This is a consequence of the flatness of the lowest conduction bands in the most space directions. The electron-mass anisotropy in the $2H$ and $3H$ ($3C$) polytypes at M (X) or K is much smaller. The findings for the conduction-band masses have consequences for the electron mobility, since this property is proportional to the inverse mass. We expect that at least for the mostly available $6H$- and $4H$-SiC polytypes, the current directions should be carefully selected. Otherwise, too small electron mobilities result. It is noteworthy to mention that the conduction-band masses given for $3H$ in Table IV cannot be indentified with the masses for the real electron motion in $3C$. The directions are not equivalent, since X_{fcc} is mapped onto M_{hex} in a neighboring BZ. For $3C$ we find for the $X\Gamma$ and XU directions $m_{||} = 0.67m_0$ or $m_\perp = 0.25m_0$. In order to prove our results, the inverse effective-mass tensor for zinc blende is transformed into the hexagonal coordinate system. Indeed, we derive the same diagonal elements as calculated for $3H$. However, this inverse effective-mass tensor is not diagonal. The experimental values for zinc-blende SiC, derived from cyclotron-resonance measurements,[59] are $m_{||} = 0.67m_0$ and $m_\perp = 0.25m_0$. There is an excellent agreement of experimental and theoretical values in this case.

Unfortunately, only one transverse effective mass is commonly derived from the experiment,[57,58] more strictly from a fit to IR spectra, for hexagonal structures. One observes $m_{||} = 0.22$ $(0.34)m_0$ and $m_\perp = 0.18$ $(0.24)m_0$ for $4H$-($6H$-)SiC. Data for $2H$ are not available. In contrast to the $3C$ case, a remarkable discrepancy appears for $6H$ and $4H$. The theoretical masses $m_{||}$ ($m_{\perp 2}$) overestimate (underestimate) the values derived from IR experiments. The third mass $m_{\perp 1}$ can hardly be identified with experimental data. A reason is due to the description[57,58] of the nitrogen donor within the simplified effective-mass approximation of Gerlach and Pollmann[61] where, moreover, only two independent components of the effective-mass tensor are assumed. On the other hand, there are also values from Faraday-rotation measurements of $6H$-SiC,[60] $m_{||} = 1.5m_0$ and $m_\perp = 0.25m_0$. In the light of the calculated masses a reinterpretation of the experimental findings in terms of the complete effective-mass tensor should be necessary.

The small spin-orbit splitting in SiC (Ref. 54) has consequences for the dispersion of the valence bands near Γ, especially in the zinc-blende case. This can be clearly seen from the calculated VBM in Fig. 1 where the spin-orbit interaction is completely neglected. There should be a tendency for nonparabolicity in the heavy-hole and light-hole bands. Nevertheless, in Table V we represent the dispersion of the Γ_{6v} heavy-hole and light-hole bands as well as the Γ_{1v} splitoff band by effective masses in important space directions ΓA, ΓK, and ΓM. We observe a remarkable anisotropy and rather different curvatures of the three bands near $\mathbf{k} = 0$. The dispersion of the heavy-hole band is rather weak. In all space directions the effective masses are larger than the free-electron mass. Apart from the ΓA direction, the band masses remark-

TABLE IV. Effective masses of electrons in the conduction-band minima. For explanations see text. All values in units of the free-electron mass m_0.

Mass	$3H$	$6H$	$4H$	$2H$
$m_{\|\|}$	0.42	0.68	0.62	0.44
$m_{\perp 1}$	0.30	1.25	0.39	0.26
$m_{\perp 2}$	0.24	0.13	0.13	0.43

TABLE V. Effective masses of holes in the three uppermost valence bands (in units of the free-electron mass).

Band	3H			6H			4H			2H		
	ΓA	ΓK	ΓM	ΓA	ΓK	ΓM	ΓA	ΓK	ΓM	ΓA	ΓK	ΓM
heavy-hole	1.87	10.73	2.75	1.83	2.26	6.11	1.73	2.41	4.23	1.64	2.26	2.75
light-hole	1.87	0.64	1.00	1.83	1.03	0.87	1.73	0.77	0.45	1.64	0.46	0.40
splitoff	0.23	0.27	0.26	0.22	0.56	0.44	0.21	0.51	0.74	0.21	0.79	1.00

ably decrease for the light-hole band and especially for the splitoff band. In contrast to the holes in the heavy-hole and light-hole bands an observable hole mobility can be only expected for the splitoff valence band.

IV. SUMMARY

In conclusion, DFT-LDA band structures of the different SiC polytypes $3H(3C)$, $6H$, $4H$, and $2H$ have been presented and discussed. The band structures result from a calculation, using the atomic coordinates from the same DFT-LDA theory as input. The ordering of the conduction-band minima is stated more precisely. We show that the minima are indeed at X ($3C$), M ($4H$, $3H$), and K ($2H$), respectively. However, the minimum in the $6H$ structure is slightly displaced from the M point towards L. Adding quasiparticle corrections to the gaps, we explain not only the physical reasons of the empirical Choyke-Hamilton-Patrick rule, but also the correct magnitude of the transition energies. Effective masses of the electrons are calculated. Their trends versus the polytypes and consequences for the electron mobility are discussed. Valence-band parameters are also derived. A comparably large crystal-field splitting and nonparabolicity are concluded in the case of the hexagonal polytypes.

ACKNOWLEDGMENTS

The work was supported by the Sonderforschungsbereich 196 (project A08) of the Deutsche Forschungsgemeinschaft and the EC Programme Human Capital and Mobility under Contract No. ERBCHRXCT 930337.

[1] W.J. Choyke, D.R. Hamilton, and L. Patrick, Phys. Rev. **133**, 1163 (1964).
[2] N. Churcher, K. Kune, and V. Heine, Solid State Commun. **56**, 177 (1980).
[3] P.J.H. Denteneer and W. van Haeringen, Phys. Rev. B **33**, 2831 (1986).
[4] P.E. Van Camp, V.E. Van Doren, and J.T. Devreese, Phys. Status Solidi B **146**, 573 (1988).
[5] K.J. Chang and M.L. Cohen, Phys. Rev. B **35**, 8196 (1987).
[6] W.R.L. Lambrecht, B. Segall, M. Methfessel, and M. van Schilfgaarde, Phys. Rev. B **44**, 3685 (1991).
[7] P.J.H. Denteneer and W. van Haeringen, Solid State Commun. **65**, 115 (1988).
[8] C. Cheng, R.J. Needs, V. Heine, and N. Churcher, Europhys. Lett. **3**, 475 (1987); J. Phys. C **21**, 1049 (1988).
[9] C. Cheng, V. Heine, and R.J. Needs, J. Phys. Condens. Matter **2**, 5115 (1990).
[10] B. Wenzien, P. Käckell, and F. Bechstedt, Surf. Sci. **307-309**, 989 (1994).
[11] P. Käckell, B. Wenzien, and F. Bechstedt (unpublished).
[12] P.J.H. Denteneer, Ph.D. thesis, Eindhoven, 1987.
[13] B.H. Cheong, K.J. Chang, and M.L. Cohen, Phys. Rev. B **44**, 1053 (1991).
[14] B. Wenzien, P. Käckell, and F. Bechstedt, in *Proceedings of the 5th International Conference on Silicon Carbide and Related Materials, Washington, 1993*, edited by M. Spencer (Institute of Physics, London, 1994).
[15] C.H. Park, B.-H. Cheong, K.-H. Lee, and K.J. Chang, Phys. Rev. B **49**, 4485 (1994).
[16] M.S. Hybertsen and S.G. Louie, Phys. Rev. B **34**, 5390 (1986).
[17] F. Bechstedt, Adv. Solid State Phys. **32**, 161 (1992).
[18] F. Bechstedt and R. Del Sole, Phys. Rev. B **38**, 7710 (1988).
[19] F. Bechstedt and R. Del Sole, in *Proceedings of the 19th International Conference on Physics and Semiconductors, Warsaw, 1988*, edited by W. Zawadzki (Institute of Physics, Polish Academy of Science, Warsaw, 1988).
[20] M. Rohlfing, P. Krüger, and J. Pollmann, Phys. Rev. B **48**, 17 791 (1993).
[21] V.I. Gavrilenko, A.V. Postnikov, N.I. Klyui, and V.G. Litovchenko, Phys. Status Solidi B **162**, 477 (1990).
[22] W.R.L. Lambrecht and B. Segall, in *Wide Band-Gap Semiconductors*, edited by T. D. Moustakas, J. I. Pankove, and Y. Hamakawa, MRS Symposia Proceedings No. 242 (Materials Research Society, Pittsburgh, 1992), p. 367.
[23] V.I. Gavrilenko, S.I. Frolov, and N.I. Klyui, Physica B **185**, 394 (1993).
[24] L. Wenchang, Z. Kaiming, and X. Xide, J. Phys. Condens. Matter **5**, 883 (1993).
[25] H.J. Junginger and W. van Haeringen, Phys. Status Solidi **37**, 709 (1970).
[26] L.A. Hemstreet and C.Y. Fong, in *Proceedings of the 3rd International Conference on Silicon Carbide, Miami Beach, 1973*, edited by R.C. Marshall, J.W. Faust, and C.Y. Ryan (University of South Carolina Press, Columbia, 1974), p. 284.
[27] A.R. Lubinsky, D.E. Ellis, and G.S. Painter, Phys. Rev. B **11**, 1537 (1975).
[28] M.-Z. Huang and W.Y. Ching, J. Phys. Chem. Solids **46**, 977 (1985).
[29] Y. Li and P.J. Lin-Chung, Phys. Rev. B **36**, 1130 (1987).

[30] W.H. Backes, P.A. Bobbert, and W. van Haeringen, Phys. Rev. B **49**, 7564 (1994).
[31] G. Wiech, in *Soft X-ray Band Spectra and Electron Structures of Metallic Materials,* edited by D.J. Fabian (Academic, London, 1968), p. 59.
[32] I.I. Shukova, V.A. Fomishev, A.S. Vinogradov, and T.M. Simkina, Fiz. Tverd. Tela (Leningrad) **10**, 1383 (1968) (in Russian).
[33] H. Hoechst, M. Tang, B.C. Johnson, J.M. Meese, G.W. Zajac, and T. H. Fleisch, J. Vac. Sci. Technol. A **5**, 1640 (1987).
[34] V. Fiorentini, Phys. Rev. B **46**, 2086 (1992).
[35] G.B. Bachelet, D.R. Hamann, and M. Schlüter, Phys. Rev. B **26**, 4199 (1982).
[36] L. Kleinman and D.M. Bylander, Phys. Rev. Lett. **48**, 1425 (1982).
[37] R. Stumpf, X. Gonze, and M. Scheffler (unpublished); X. Gonze, R. Stumpf, and M. Scheffler, Phys. Rev. B **44**, 8503 (1991).
[38] P.J.H. Denteneer, C.G. Van de Walle, and S.T. Pantelides, Phys. Rev. B **39**, 10 809 (1989).
[39] R. Stumpf and M. Scheffler, Comput. Phys. Commun. **79**, 447 (1994).
[40] R. Car and M. Parrinello, Phys. Rev. Lett. **55**, 2471 (1985).
[41] D.J. Chadi and M.L. Cohen, Phys. Rev. B **8**, 5747 (1973).
[42] R.A. Evarestov and V.P. Smirnov, Phys. Status Solidi B **119**, 9 (1983).
[43] D.M. Ceperley and B.A. Alder, Phys. Rev. Lett. **45**, 566 (1980).
[44] J.P. Perdew and A. Zunger, Phys. Rev. B **23**, 5048 (1981).
[45] R.W.G. Wyckhoff, *Crystal Structures* (Interscience, New York, 1964), Vol. 1.
[46] R.F. Adamsky and K.M. Merz, Z. Kristallogr. **111**, 350 (1950).
[47] A.H. Gomes de Mesquita, Acta Crystallogr. **23**, 610 (1967).
[48] *Numerical Data and Functional Relationships in Science and Technology,* edited by K.-H. Hellwege and O. Madelung, Landolt-Börnstein, New Series, Group III, Vol. 17, Pt. a (Springer, Berlin, 1982); *ibid.*, Vol. 22, Pt. a (1986).
[49] H. Schulz and K.H. Thiemann, Solid State Commun. **32**, 783 (1979).
[50] L. Hedin, Phys. Rev. **139**, A796 (1965).
[51] W.A. Harrison, *Electronic Structure and the Properties of Solids* (Freeman, San Francisco, 1980).
[52] M.R. Salehpour and S. Satpathy, Phys. Rev. B **41**, 3048 (1990).
[53] P.J. Denteneer (unpublished).
[54] R.G. Humphreys, D. Bimberg, and W.J. Choyke, Solid State Commun. **39**, 163 (1981).
[55] M. Murayama and T. Nakayama, Phys. Rev. B **49**, 4710 (1994).
[56] W. Mönch, *Proceedings of the 1st International Symposium Control of Semiconductor Interfaces* (Karuizawa, Japan, 1993).
[57] W. Suttrop, G. Pensl, W.J. Choyke, R. Stein, and S. Leibenzeder, J. Appl. Phys. **72**, 3708 (1992).
[58] W. Götz, A. Schöner, G. Pensl, W. Suttrop, W.J. Choyke, R. Stein, and S. Leibenzeder, J. Appl. Phys. **73**, 3332 (1993).
[59] R. Kaplan, R.J. Wagner, H.J. Kim, and R.F. Davis, Solid State Commun. **55**, 67 (1985).
[60] B. Ellis and T.S. Moss, Proc. R. Soc. London Ser. A **299**, 383 (1967); **299**, 393 (1967).
[61] B. Gerlach and J. Pollmann, Phys. Status Solidi B **67**, 93 (1975).